JOURNAL OF MATERIALS SCIENCE 27 (1992) 1327–1331

# CSL descriptions of rhombohedral twinning in $TlBiTe_2$

E. G. DONI, E. K. POLYCHRONIADIS
*Solid State Section 313-1, Department of Physics, Aristotle University of Thessaloniki, 54006 Thessaloniki, Greece*

Rhombohedral twins of the ternary semiconductor $TlBiTe_2$ have been studied and it has been found that they were either coherent or non-coherent. By an appropriate approximation of the rhombohedral angle by a pair of integers $p$ and $q$, the rhombohedral twins can be described by the coincidence site lattice (CSL) model. Since the best description for reflection twins is to note the lattice plane $(h\,k\,l)$ acting as a mirror plane, the $(h\,k\,l)$ description has been used. It has been found that the coherent twins are described by a CSL with low multiplicity $\Sigma$, and the non-coherent ones by a CSL with high multiplicity $\Sigma$.

## 1. Introduction

The coincidence site lattice (CSL) model has been proved to be a very useful tool for the study of grain boundaries (GBs) in materials. The idea of the CSL model was introduced by Friedel [1] in the case of the twin relationship of a bicrystal and later its general applicability has been discussed [2]. A lot of publications have appeared concerning the use of the CSL model for the characterization of the bicrystal rotation relationship and numerical solutions for the systematic derivation of the CSLs of the cubic and hexagonal systems [3–11].

The application of the CSL description to the rhombohedral twinning in $TlBiTe_2$ has particular interest as the CSL model has to be adapted to two kinds of reflection twin, i.e. the coherent and non-coherent ones. In the first kind the mirror plane is a crystallographic plane while in the second it is not. The ternary semiconductor $TlBiTe_2$ is a characteristic rhombohedral material because it is considered "pseudocubic" as it can be described by a multiple rhombohedral cell having an almost 90° rhombohedral angle (88°21′). Therefore the interpretation of its almost cubic diffraction patterns is easy and the analysis of the observed twins is made by using the rhombohedral description without going into the complexity of the hexagonal one.

In the light of the above considerations, the aim of the present work is to combine some theoretical results with the experimental information, in order to classify, according to the CSL model, the rhombohedral twins in $TlBiTe_2$.

## 2. Evolution of the CSL model in rhombohedral symmetry

A systematic study of the CSLs of the rhombohedral system appeared some years ago [12]. In that paper the rhombohedral angle $\alpha$ was approximated by two integer numbers $p, q$, according to the relation

$$\tan^2(\alpha/2) = p/q \qquad (p, q) \div 1^* \tag{1}$$

The analytical expressions for the CSL multiplicity function $\Sigma$, the CSL rotation matrix elements and the angles and the rotation axis indices of the six symmetrically equivalent descriptions of the same CSL were constructed in direct and reciprocal space, as a function of the rotation axis indices $[u\,v\,w]$ and some integer parameters. The general CSL rotation matrix $R$ is written in the form

$$R = (1/\Sigma)[r_{ij}] \qquad i, j = 1, 2, 3 \tag{2}$$

where $\Sigma$ and $r_{ij}$ are integers without a common divisor. $\Sigma$ is the multiplicity of the CSL, i.e. the ratio of the volume of the CSL unit cell over the volume of the (parent) lattice unit cell. The matrix $R$ expresses a rotation in the coordinate system of the (parent) lattice.

In order to describe the reflection twins we usually note the mirror plane indices $(h\,k\,l)$. In the case of coherent twins the mirror plane is a low-indexed lattice plane, which is part of the CSL. In the case of non-coherent twins the mirror plane is not a crystallographic plane. Therefore the derivation of the CSL rotation matrix $\tilde{R}$ as a function of the mirror plane indices $(h\,k\,l)$ becomes essential. The analytical expressions for the elements of this matrix are

$$\begin{aligned}
\tilde{r}_{11} &= [2qh + (k + l)(p - q)]h - \tilde{d} \\
\tilde{r}_{12} &= [2qh + (k + l)(p - q)]k \\
\tilde{r}_{13} &= [2qh + (k + l)(p - q)]l \\
\tilde{r}_{21} &= [2qk + (h + l)(p - q)]h \\
\tilde{r}_{22} &= [2qk + (h + l)(p - q)]k - \tilde{d} \\
\tilde{r}_{23} &= [2qk + (h + l)(p - q)]l \\
\tilde{r}_{31} &= [2ql + (k + h)(p - q)]h \\
\tilde{r}_{32} &= [2ql + (k + h)(p - q)]k \\
\tilde{r}_{33} &= [2ql + (k + h)(p - q)]l - \tilde{d}
\end{aligned} \tag{3}$$

* $(x, y) \div z$ means that the greatest common divisor of $x, y$ is $z$.

0022–2461 

where the rhombohedral angle $\alpha$ is approximated by Equation 1 and $\tilde{d}$, which is the CSL generating function, is given by the relation

$$\tilde{d} = q(h^2 + k^2 + l^2) + (p - q)(hk + lh + kl) \quad (4)$$

as an integer function. The preserved character of the CSL generating function allows the generation of CSLs on the basis of the mirror plane descriptions. By considering the symmetrically equivalent descriptions of one and the same CSL [12] we may complete the study of the CSLs of the rhombohedral system. Therefore the generation and the analysis of the rhombohedral CSLs can be easily handled computationally.

Moreover, the simple form of the matrix elements (Equations 3) and of the CSL generating function (Equation 4) allows a direct examination of twins with low $(h\,k\,l)$ indices. For example, if $(h\,k\,l) = (1\,0\,0)$, then

$$\tilde{d} = q \quad (5)$$

and

$$\tilde{R} = \left(\frac{1}{q}\right)\begin{bmatrix} q & 0 & 0 \\ p-q & -q & 0 \\ p-q & 0 & -q \end{bmatrix} \quad (6)$$

Therefore since $\tilde{d}$ and the elements of the matrix $\tilde{R}$ (Equations 5 and 6) do not have any common divisor, it is obvious that $\Sigma = q$.

If $(h\,k\,l) = (1\,1\,0)$, it holds that

$$\tilde{d} = p + q \quad (7)$$

and

$$\tilde{R} = \left(\frac{1}{p+q}\right)\begin{bmatrix} 0 & p+q & 0 \\ p+q & 0 & 0 \\ 2(p-q) & 2(p-q) & -(p+q) \end{bmatrix} \quad (8)$$

A possible common factor between the CSL generating function $\tilde{d}$ and the elements of the matrix $\tilde{R}$ (Equations 7 and 8) is the number 2. Therefore, in this case, either $\Sigma = p + q$ or $\Sigma = (p + q)/2$.

In the case where $(h\,k\,l) = (1\,1\,1)$, since $p$ and $q$ are eliminated between the matrix elements (Equations 3) and the expression giving $\tilde{d}$ (Equation 4), it is obvious that the CSLs produced are independent of the values of $p$ and $q$.

## 3. Structural considerations for $TlBiTe_2$

$TlBiTe_2$ has at room temperature an NaCl-type structure which has a slight rhombohedral distortion with an elongation along the threefold [1 1 1] axis. There is also an ordering of successive layers normal to the rhombohedral axis in the sequence –Tl–Te–Bi–Te–Tl–. Hockings and White [13] have found that the lattice parameter of the primitive cell, which has four atoms, is $a_0 = 0.8137$ nm and the rhombohedral angle is $\alpha = 32° 18'$.

The same structure can also be described by a non-primitive (or multiple) rhombohedral cell which is the pseudocubic one. The multiple cell has 64 atoms, a lattice parameter of $a_0 = 1.2988$ nm and a rhombohedral angle $\alpha = 88° 21'$ [14].

There is a direct relationship between the two cells. From the geometry of the lattice the following relations are revealed:

$$\begin{aligned} a_p &= \frac{1}{2}a_m + \frac{1}{4}b_m + \frac{1}{4}c_m \\ b_p &= \frac{1}{4}a_m + \frac{1}{2}b_m + \frac{1}{4}c_m \\ c_p &= \frac{1}{4}a_m + \frac{1}{4}b_m + \frac{1}{2}c_m \end{aligned} \quad (9)$$

$a_p, b_p, c_p$ are the parameters of the primitive cell and $a_m, b_m, c_m$ the parameters of the corresponding multiple one. Keeping the notation of International Tables for X-ray crystallography [15], we write

$$(a_m, b_m, c_m) = (a_p, b_p, c_p)P$$

and consequently

$$(a_p, b_p, c_p) = (a_m, b_m, c_m)Q$$

where

$$P = \begin{bmatrix} 3 & -1 & -1 \\ -1 & 3 & -1 \\ -1 & -1 & 3 \end{bmatrix} \quad (10)$$

and

$$Q = \begin{bmatrix} 1/2 & 1/4 & 1/4 \\ 1/4 & 1/2 & 1/4 \\ 1/4 & 1/4 & 1/2 \end{bmatrix} \quad (11)$$

$Q$ is the matrix which transforms a vector of the primitive cell into a vector of the multiple cell. Let $R_p$ be a 180° rotation matrix, expressing a rotation described in the primitive cell reference system. This matrix is transformed to the matrix $R_m$, expressing a rotation described in the multiple-cell reference system by the similarity transformation

$$R_m = QR_pP \quad (12)$$

Similarly if $\tilde{R}_p$ is the 180° rotation matrix given as a function of the plane indices in the primitive-cell reference system, then the corresponding matrix $\tilde{R}_m$ in the multiple-cell reference system is given by the similarity transformation

$$\tilde{R}_m = P\tilde{R}_pQ \quad (13)$$

It should be noticed that according to the definition of $\Sigma$, its value remains invariant by the above similarity transformations, since the change in volume is the same for the (parent) lattice and for the CSL.

## 4. Observed twins in $TlBiTe_2$

A systematic study by transmission electron microscopy of the twins in $TlBiTe_2$ has been analytically presented in a previous paper [14]. Two kinds of twin have been observed which can be easily described by the pseudocubic cell. The first is the coherent $\{1\,0\,0\}$-type twin in which the twinning operation is determined by the (1 0 0) mirror plane or by a 180° rotation

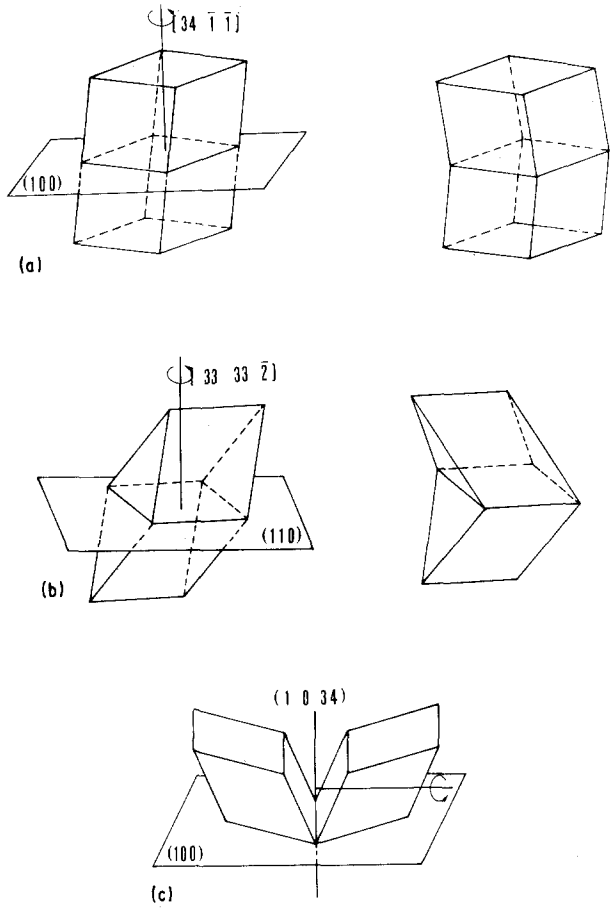


*Figure 1* Three-dimensional schematic diagrams of the observed twins in $TlBiTe_2$: (a) coherent {1 0 0} type, (b) coherent {1 1 0} type and (c) non-coherent {1 0 0} type.

axis perpendicular to it (Fig. 1a) and the coherent {1 1 0}-type twin in which the twinning operation is determined by the (1 1 0) mirror plane or by a 180° rotation axis perpendicular to it (Fig. 1b). In both these cases of coherent twins, the mirror plane descriptions have simple indices. Moreover the mirror planes are crystallographic planes. In the second kind of twin, the mirror plane is a high-indexed plane, i.e. the (1 0 34). However there is a common plane with simple indices, the (1 0 0), which is also the composition plane. Consequently this is a non-coherent twin (Fig. 1c). This is not a "classical" twin, as its reflection plane is non-crystallographic and therefore it appears with high indices. However, it is a significant defect that exists in the material, which has a great influence on its transport properties [16].

The two kinds of twin are easily identified by electron diffraction if their relative orientation to the electron beam is easily accessible using a double-tilt specimen holder. By putting the composition plane in edge-on position the row of spots perpendicular to it is unsplit, as in all three cases the composition plane is a plane common to both grains (Fig. 2). In the two cases of the first kind of twin the splitting of the other spots is parallel to the unsplit row as the composition plane is also the twin plane, while in the second kind the situation is different. As expected, due to the non-coherency the splitting is not parallel to the unsplit row, but it is easily explained by interpretation of the diffraction pattern. Therefore the two diffraction patterns arising from the two grains are constructed independently at their {1 1 0} section. Their superposition then shows an identity with the electron diffraction pattern taken from both grains (Fig. 3). According to their orientaion, only in one grain is the threefold [1 1 1] axis perpendicular to the electron beam. Consequently, the extra (1 1 1) spots due to the ordering belong to one of the twin crystals, and therefore are unsplit in the diffraction pattern.

## 5. CSL descriptions of $TlBiTe_2$ twins

As already stated, the CSL description of a rhombohedral bicrystal is based on the approximation of the rhombohedral angle by the ratio of two integer numbers according to Equation 1. Therefore the rhombohedral angle of the primitive cell of $TlBiTe_2$ has been approximated by

$$\tan^2\left(\frac{32° 18'}{2}\right) \simeq \frac{1}{12} \tag{14}$$

and the rhombohedral angle of the multiple cell by

$$\tan^2\left(\frac{88° 21'}{2}\right) \simeq \frac{16}{17} \tag{15}$$

The results concerning the symmetrically equivalent descriptions in both $(h\,k\,l)$ and $[u\,v\,w]$ indexing of each

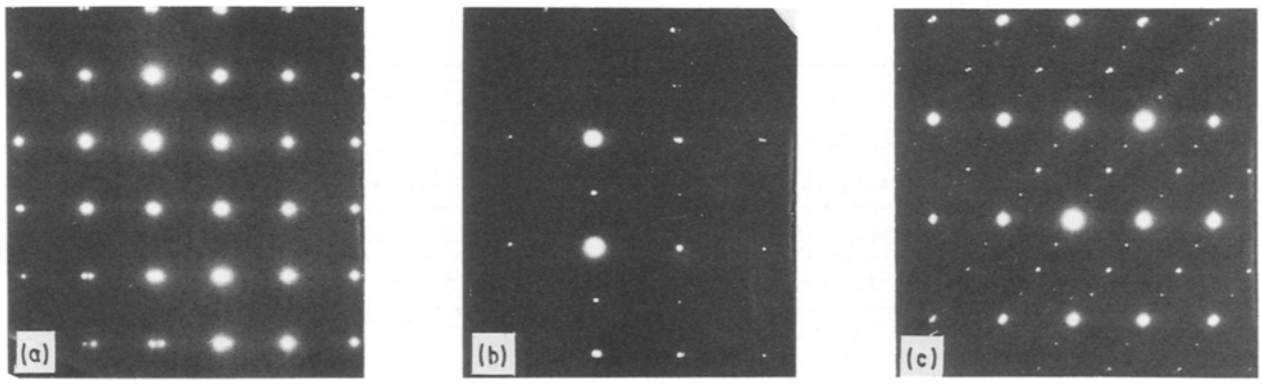


*Figure 2* Diffraction patterns of the observed twins in $TlBiTe_2$ when the composition plane is in edge-on position: (a) coherent {1 0 0} type (section (0 0 1)), (b) coherent {1 1 0} type (section (1 1̄ 2)) and (c) non-coherent {1 0 0} type (section (0 1̄ 1)). Both grains are simultaneously diffracting. The splitting of the spots due to the twin relation is visible. For the coherent types the splitting is parallel to the unsplit row, while for the non-coherent type it is not.

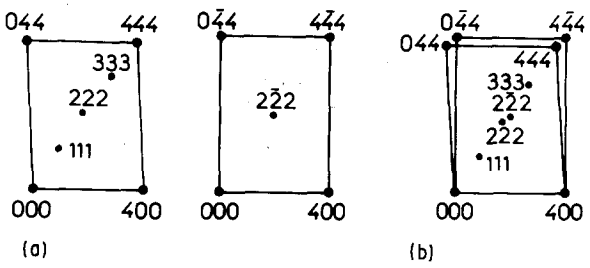


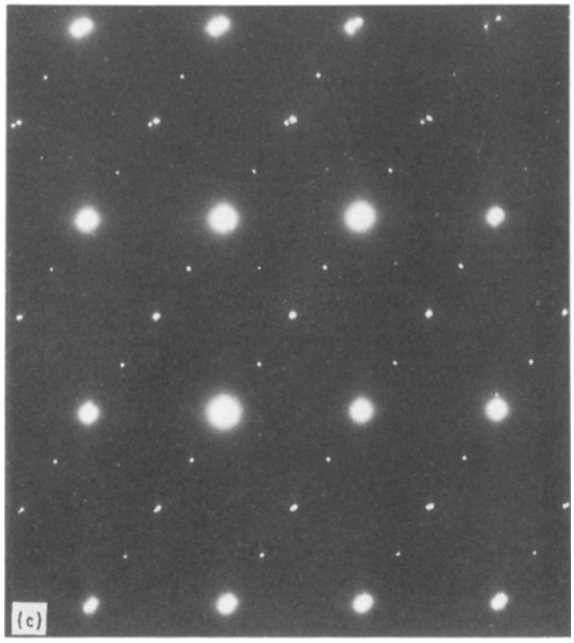


*Figure 3* (a, b) Theoretically constructed and (c) experimentally observed diffraction patterns from the non-coherent {1 0 0}-type twin when the composition {1 0 0} plane, common to both grains, is in edge-on position.

of the different kinds of twin observed are summarized in Tables I, II and III. Tables I and II are concerned with the {1 0 0}-type and {1 1 0}-type coherent twins, respectively, while Table III concerns the {1 0 0}-type non-coherent twin, all in the multiple-cell description. For each of the six symmetrically equivalent descriptions, the rotation angle θ and the $(h\,k\,l)$ and $[u\,v\,w]$ indices are given. For each description, the $(h\,k\,l)$ and $[u\,v\,w]$ indices are connected by the relations

$$\begin{aligned} u &= 2qh + (k + l)(p - q) \\ v &= 2qk + (h + l)(p - q) \\ w &= 2ql + (h + k)(p - q) \end{aligned} \tag{16}$$

The necessity to represent all the symmetrically equivalent descriptions by both the plane indices $(h\,k\,l)$ and the rotation axis indices $[u\,v\,w]$ becomes clear from the above tables. As can be easily seen in each of the symmetrically equivalent descriptions, the simple indices – when they exist – are found either in the $(h\,k\,l)$ or in the $[u\,v\,w]$ formulation. The results concerning the rotation axis indices $[u\,v\,w]$ in the primitive cell are transformed to the multiple cell by using the matrix $Q$, and the results concerning the plane indices $(h\,k\,l)$ in the primitive cell are transformed to the multiple cell by using the matrix $P$.

## 6. Discussion and conclusions

The three types of reflection twin observed in $TlBiTe_2$ can be divided into two main kinds, the coherent and the non-coherent ones. The coherent {1 0 0}- and {1 1 0}-type twins comprise a common lattice plane, i.e. the mirror plane for the two grains, which also coincides with the composition plane. Thus the mirror-plane description of the pseudocubic cell is of low

TABLE I Symmetrically equivalent descriptions in $(h\,k\,l)$ and $[u\,v\,w]$ indexing of the {1 0 0}-type coherent twin ($\Sigma = 17$)

| No. | | Primitive cell | | | | | | Multiple cell | | | | | |
|---|---|---|---|---|---|---|---|---|---|---|---|---|---|
| | θ (deg) | $h$ | $k$ | $l$ | $u$ | $v$ | $w$ | $h$ | $k$ | $l$ | $u$ | $v$ | $w$ |
| 1 | 180 | 2 | 1 | 1 | 26 | $\bar{9}$ | $\bar{9}$ | 1 | 0 | 0 | 34 | $\bar{1}$ | $\bar{1}$ |
| 2 | 121.97 | $\bar{1}$ | $\bar{1}$ | 0 | $\overline{13}$ | $\overline{13}$ | 22 | $\bar{1}$ | $\bar{1}$ | 1 | $\overline{17}$ | $\overline{17}$ | 18 |
| 3 | 121.97 | 1 | 0 | 1 | 13 | $\overline{22}$ | 13 | 1 | $\bar{1}$ | 1 | 17 | $\overline{18}$ | 17 |
| 4 | 88.32 | 9 | 9 | 17 | 1 | 1 | $\bar{3}$ | 1 | 1 | 33 | 0 | 0 | $\bar{1}$ |
| 5 | 180 | 9 | 13 | 13 | $\bar{1}$ | 1 | 1 | 1 | 17 | 17 | 0 | 1 | 1 |
| 6 | 88.32 | 9 | 17 | 9 | 1 | $\bar{3}$ | 1 | 1 | 33 | 1 | 0 | $\bar{1}$ | 0 |

TABLE II Symmetrically equivalent descriptions in $(h\,k\,l)$ and $[u\,v\,w]$ indexing of the {1 1 0}-type coherent twin ($\Sigma = 33$)

| No. | | Primitive cell | | | | | | Multiple cell | | | | | |
|---|---|---|---|---|---|---|---|---|---|---|---|---|---|
| | θ (deg) | $h$ | $k$ | $l$ | $u$ | $v$ | $w$ | $h$ | $k$ | $l$ | $u$ | $v$ | $w$ |
| 1 | 180 | 3 | 3 | 2 | 17 | 17 | $\overline{18}$ | 1 | 1 | 0 | 33 | 33 | $\bar{2}$ |
| 2 | 91.74 | $\bar{1}$ | $\bar{2}$ | $\bar{1}$ | 9 | $\overline{26}$ | 9 | 0 | $\bar{1}$ | 0 | 1 | $\overline{34}$ | 1 |
| 3 | 91.74 | 2 | 1 | 1 | 26 | $\bar{9}$ | $\bar{9}$ | 1 | 0 | 0 | 34 | $\bar{1}$ | $\bar{1}$ |
| 4 | 180 | 9 | 9 | 17 | 1 | 1 | $\bar{3}$ | 1 | 1 | 33 | 0 | 0 | $\bar{1}$ |
| 5 | 118.02 | 1 | 17 | 17 | $\bar{5}$ | 3 | 3 | 31 | 33 | 33 | $\bar{1}$ | 1 | 1 |
| 6 | 118.02 | 17 | 1 | 17 | 3 | $\bar{5}$ | 3 | 33 | 31 | 33 | 1 | $\bar{1}$ | 1 |

TABLE III Symmetrically equivalent descriptions in $(h\,k\,l)$ and $[u\,v\,w]$ indexing of the $\{1\,0\,0\}$-type non-coherent twin ($\Sigma = 561$)

| No. | | Primitive cell | | | | | | Multiple cell | | | | | |
|---|---|---|---|---|---|---|---|---|---|---|---|---|---|
| | θ (deg) | $h$ | $k$ | $l$ | $u$ | $v$ | $w$ | $h$ | $k$ | $l$ | $u$ | $v$ | $w$ |
| 1 | 180 | $\overline{36}$ | 35 | $\overline{69}$ | $\overline{8}$ | $\overline{9}$ | $\overline{25}$ | $\overline{1}$ | 0 | $\overline{34}$ | 0 | $\overline{1}$ | $\overline{33}$ |
| 2 | 120.06 | $\overline{35}$ | $\overline{1}$ | $\overline{34}$ | $\overline{13}$ | 21 | $\overline{12}$ | $\overline{35}$ | 33 | $\overline{33}$ | $\overline{17}$ | 17 | $\overline{16}$ |
| 3 | 120.06 | 1 | 34 | 35 | $\overline{21}$ | 12 | 13 | $\overline{33}$ | 33 | 35 | $\overline{17}$ | 16 | 17 |
| 4 | 177.58 | 25 | 25 | 17 | 69 | 69 | $\overline{71}$ | 33 | 33 | 1 | $\overline{34}$ | 34 | $\overline{1}$ |
| 5 | 88.26 | $\overline{2}$ | $\overline{1}$ | $\overline{1}$ | $\overline{26}$ | 9 | 9 | $\overline{1}$ | 0 | 0 | $\overline{34}$ | 1 | 1 |
| 6 | 91.69 | 9 | 17 | 9 | 1 | $\overline{3}$ | 1 | 1 | 33 | 1 | 0 | $\overline{1}$ | 0 |

indices. The non-coherent $\{1\,0\,0\}$ type has a common lattice plane, the composition plane, which is not the mirror plane of the twinning. In this case the mirror plane has no low indices.

The twins in $TlBiTe_2$ presented above have been described by the CSL model. This was the main purpose of the present work. The CSL descriptions were achieved by an appropriate approximation of the rhombohedral angle by a pair of integers, $p$ and $q$, and the analysis presented. From Tables I, II and III it is concluded that the coherent-type twins are described by low $\Sigma$-value CSLs, i.e. $\Sigma = 17$ and 33, in contrast to the non-coherent type which exhibits a very large multiplicity, i.e. $\Sigma = 561$. This behaviour is attributed to the fact that in this case the mirror plane is not a crystallographic plane.

## Acknowledgements

This work has been supported by the EEC under stimulation contract No. ST2J-0289-C. The authors gratefully acknowledge Professors Th. Karakostas and G. L. Bleris for helpful discussions during the course of this study.

## References

1. G. FRIEDEL, "Lecons de Cristallographie" (Blanchard, Paris, reprinted 1964).
2. M. L. KRONBERG and F. H. WILSON, *Trans. TMS–AIME* **185** (1949) 501.
3. H. GRIMMER, W. BOLLMANN and D. H. WARRINGTON, *Acta Crystallogr.* **A30** (1974) 197.
4. D. H. WARRINGTON, *J. Phys. (Paris) Colloq.* **36** (C4) (1975) 87.
5. R. BONNET, E. COUSINEAU and D. H. WARRINGTON, *Acta Crystallogr.* **A37** (1981) 184.
6. G. L. BLERIS and P. DELAVIGNETTE, *ibid.* **A37** (1981) 779.
7. G. L. BLERIS, G. NOUET, S. HAGEGE and P. DELAVIGNETTE, *ibid.* **A38** (1982) 550.
8. P. DELAVIGNETTE, *J. Phys. (Paris) Colloq.* **43** (C6) (1982) 1.
9. S. HAGEGE and G. NOUET, *Scripta Metall.* **17** (1983) 1095.
10. G. L. BLERIS, Th. KARAKOSTAS and P. DELAVIGNETTE, *Comput. Phys. Commun.* **28** (1983) 287.
11. G. L. BLERIS, E.G. DONI, Th. KARAKOSTAS, J. G. ANTONOPOULOS and P. DELAVIGNETTE, *Acta Crystallogr.* **A41** (1985) 445.
12. E. G. DONI, Ch. FANIDES and G. L. BLERIS, *Cryst. Res. Techn.* **21** (1986) 1469.
13. E. F. HOCKINGS and J. G. WHITE, *Acta Crystallogr.* **14** (1961) 328.
14. E. K. POLYCHRONIADIS and J. STOEMENOS, *J. Mater. Sci.* **17** (1982) 2077.
15. "International Tables for X-ray Crystallography", Vol. A (Reidel, Boston, 1983) p. 70.
16. O. VALASSIADES, E. K. POLYCHRONIADIS, J. STOEMENOS and N. A. ECONOMOU, *Phys. Status Solidi (a)* **65** (1981) 215.

*Received 20 December 1990*
*and accepted 13 May 1991*